Characterization Studies on Photo Conductance, Dielectric Studies and Homo-Lumo Analysis of Synthezed of 4-Nitrophenol Single Crystal

S. Ayyappan[1*]& Gokila A[2]
[*]Government College of Engineering, Salem

Corresponding author: **Dr. S. Ayyappan**

Abstract: A comprehensive characterization of single-crystal 4-nitrophenol (4NP) was conducted using a multi-technique approach. The crystal's structure and crystallinity were confirmed through X-ray Diffraction (XRD) analysis. Fourier Transform Infrared Spectroscopy (FT-IR) was employed to assess the vibration modes of functional groups. UV-Vis-NIR spectroscopy provided insights into the crystal's optical properties. Thermal stability was evaluated using Thermogravimetric Analysis (TGA) and Differential Scanning Calorimetry (DSC). Dielectric and photoconductance tests were conducted to assess electrical properties. Second harmonic efficiency, found to be 7.81 times greater than standard KDP, was measured to understand nonlinear optical behavior. Photoluminescence studies were performed to explore light emission properties. Additionally, investigations into HOMO-LUMO energy levels and first hyperpolarizability were conducted to further characterize the crystal's electronic structure and nonlinear optical potential of the 4-nitrophenol samples.

Keywords: 4-nitrophenol, Thermal stability, Photoluminescence, Hyperpolarizability,Homo –Lumo

1. Introduction

The Salts may be framed with a variety of natural and artificial bases thanks to phenolic ink OH. Recently described compounds include trinitrophenol methyl p-hydroxybenzoate, L-histidine onium-4-nitrophenol, 4-nitrophenol 4-nitrophenoldimethy - laminopyridinium, L-arginine, and 4-nitrophenol-4-nitrophenol dihydride, To achieve polarisation of the polymer, the material should increase the number of α-electrons and the length of delocalization. 4-Nitrophenol is a bipolar chromophore with a substantial amount of reactivity and a highly delocated form framework linking the donor to the source.[1]These facts led to the production of

single gems of 4-nitrophenol using the slow vanishing arrangement development technique. The process was discussed, and the results were evaluated.

Because it is a transparent phenolic chemical that includes both nitro (acceptor bunch) and a hydroxyl (donor bunch) on a benzene ring, 4-nitrophenol (4NP) is a captivating substance. Due to the 4NP's excellent dipolar chromophore and patron π-acceptor system (D-π- A), its sub-nuclear hyperpolarizability can increase due to the more likely potential of proton transfer from phenolic (OH) to diverse regular bases.[2]On the other hand, it is also suggested to synthesise or electrochemically reduce 4-NP to 4-aminophenol.[3] Whatever the case, these approaches can produce distinctively scented species that are just as hazardous as or even more so as 4-NP. For instance, 4-nitrocathechol, hydroquinone, p-benzoquinone, or phenol [4-6].It must have strong second request hyperpolarizability (β) [7].The single crystals of 4-nitrophenol are formed based on these facts. Findings were reported, and the outcomes were assessed.

2. Synthesis of Organic Crystal 4-Nitrophenol

The commercially viable 4-Nitrophenol reactants (Merck 99%) were dissolved in acetone and thoroughly agitated for about 20 minutes. The solutions were then mixed and agitated using a magnetic stirrer for about an hour. Two filters of Whatman filter paper, grade 42, are applied to a saturated solution before being transferred to a 250 ml beaker. To control the rate at which the solvent vaporises, cover the beaker with a thin plastic panel and store it somewhere unappealing. High-quality crystals were added to the mother liquor after four days. The crystal consistency is depicted in Figure 1.

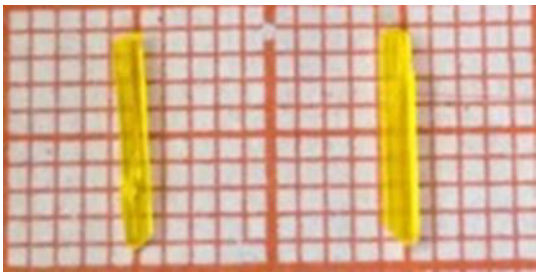

Figure 1.Crystal 4-nitrophenol

3. Result and Discussion

3.1. XRDof4-Nitrophenol Single Crystal

A single crystal XRD, fitted with the sapphire CCD detector and an improved diffractometer (MoKα radiation graphite monochromator, μ) was performed on the 4NP original single crystal using Oxford diffraction Xcalibur. The findings indicate that the title compound for the $P2_1/c$ space group pertains to the monoclinic. The lattice constant values are a = 6.16 Å, b = 8.83 Å and c =11.54 Å.

3.2. Powder XRD Analysis

A powder X-ray diffraction pattern was performed on the generated crystal using a Rich Seifert diffractometer. The scintilation counter is used to gather diffraction pattern data, which is then detected by a diffractometer equipped with monochromatic CuKα radiation (1.540598A). The growing crystals are ground into a fine powder and examined. Scan the sample in the range of 2 digits from 5 to 800 at a rate of 3 scans per minute. A 4NP crystal powder X-ray picture can be seen in Figure 2. The crystal-clear Bragg peak with a distinct 2-cm angle demonstrates the sample's clarity. Maximum intensity matching to the (122) plane is 5153 counts per second. TREOR 90 is used to programme various reflection planes (hkl).

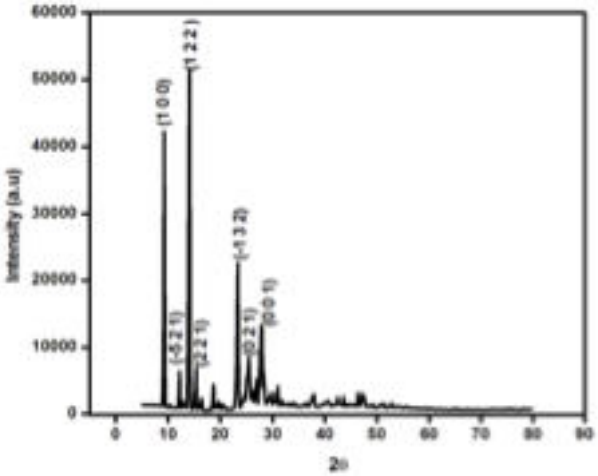

Figure 2. Powder XRD spectrum of 4NP crystal

3.3. Optical Studies

Using a Perkin-Elmer Lambda 35 spectrophotometer, the transmission spectra of the developing crystal in the wavelength range of 200 to 1200 nm was captured. The spectrum as seen is shown in Figure 3. The growing crystal has a wider spectrum of transparency in the visible and near infrared. This figure shows the crystal's ultraviolet wavelength, which is connected to the aromatic region of the crystal's π-π* transition. The strong visible light crystal transmission obtained makes it simple for opto-electronic applications to develop into a potential crystal. The produced crystal is more than 97% transparent and 470–1100 nm in wavelength. The solution-grown 4NP crystal's excellent light transmission may be a result of the limited number of defects and the lack of inclusions. This decreases the dispersion and increases the production strength of the 4NP crystal [8-10]. The optical absorption coefficient (α) was calculated from the transmittance using the given formula

$$\alpha = \frac{2.3036 \log (1/T)}{d}$$

Where T is the measured crystal transmittance and d is the thickness of the sample. Assuming parabolic trends, the relation between α and Eg is given by

$$\alpha = \frac{A(h\upsilon - E_g)^n}{h\upsilon}$$

Where A is a constant, E_g is the optical band gap of the material, υ is the frequency of the incident photon and h is the planks constant. Figure 4 shows the plot of hυ and $(\alpha h\upsilon)^2$. By extrapolating the linear part in the graph of $(\alpha h\upsilon)^2$ and sample the optical band gap of the material is obtained. It was found that the optical band gap was 2.97 eV. Wide-band crystals with a higher threshold for laser damage and transmission in the visible field oflight are predicted to have higher [11,12].

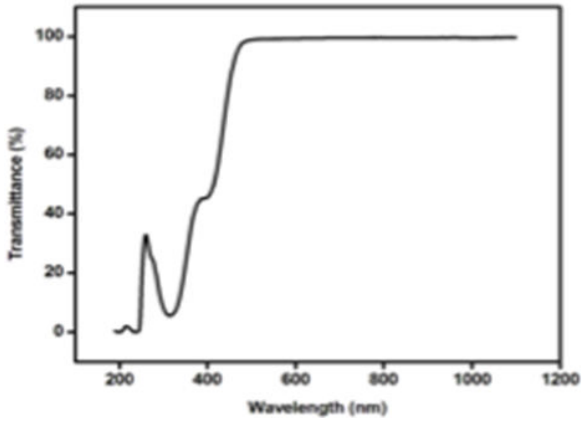

Figure3. Optical transmittance spectrum of 4NP crystal

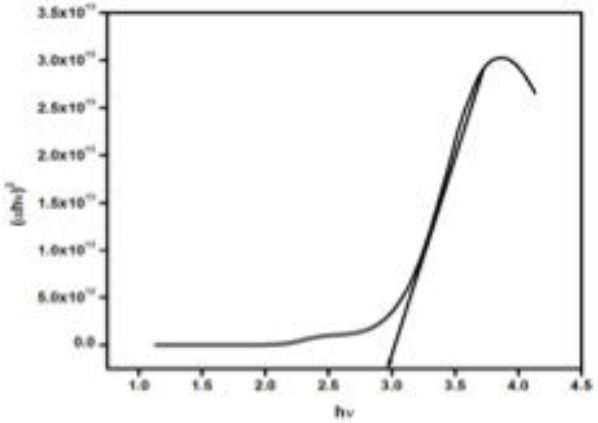

Figure 4. Plot of hυ Vs $(\alpha h\upsilon)^2$ 4NP crystal

3.4. Dielectric Studies

Dielectric measurement is crucial for the investigation of lattice dynamics. The existence of atoms, defects, ions and their bonds, and the mechanism of material polarisation are all valuable information that is provided. The crystal's electro-optical properties and its dielectric properties are frequently connected. The generated crystal's dielectric analysis was performed using an HIOKI LCR HITESTER (model 3532-50). Temperatures between 303K and 335K are used for the experiments. The crystal should be positioned between two copper plates to provide a parallel capacitance that can be measured. The crystal's capacitance is calculated by shifting the frequency range from 50Hz to 5MHz. Calculate the crystal's dielectric constant using the capacitance value that was obtained using the equation.

$$\varepsilon_r = \frac{Cd}{\varepsilon_o A}(1)$$

Where C is the measured capacitance, d is the thickness of the crystal, A is the cross-sectional area of the crystal and ε_o is the free space permittivity of the crystal. Figure 5.a shows the relation between the dielectric constant and the growing crystal frequency. This graph demonstrates that the dielectric constant is higher at low frequencies and that it rises with increasing temperature. As the frequency rises, the dielectric constant value falls and becomes constant at very high frequencies. Dielectric constant knowledge is gained from dielectric research. As a result, various polarizations are brought about by electrons, ions, space load, and orientation. Among these polarizations, the polarisation of the space load takes sample integrity and purity into account. As a result, it works well in the current system at both high temperatures and low frequencies [13-15].The generated crystal's frequency-dependent dielectric loss is shown in Figure 5. At high frequencies, the dielectric loss is quite small. This low value suggests that crystals are of superior quality and have fewer flaws, making them a desirable contender for optoelectronic applications[16,17]. To enhance the SHG coefficient for a reduced dielectric constant at high frequencies, Miller's law offers a useful parameter [18]. Recent research suggests that formed crystals have a low dielectric constant. This is an important property for electrostatic and microelectronic applications[19, 20].

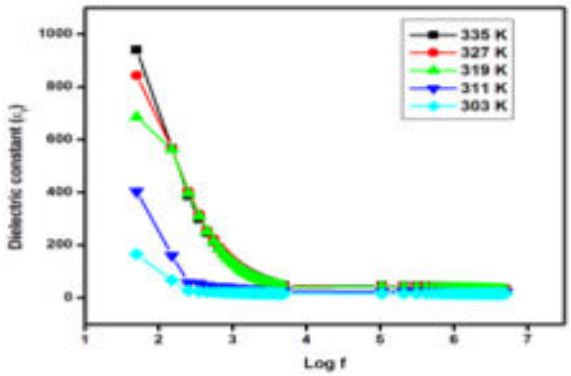

Figure 5.a Dielectric constant Vs frequency of 4NP crystal

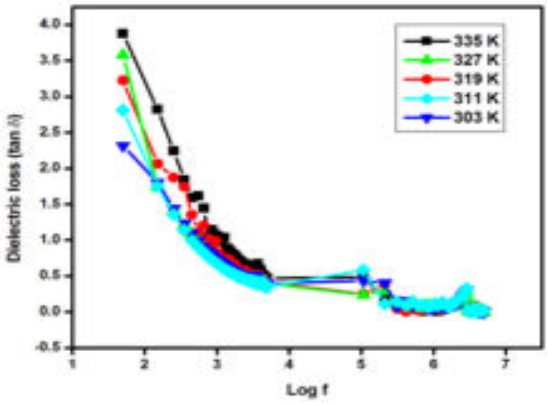

Figure 5.b Dielectric loss Vs frequency of 4NP crystal

3.5. Photoconductivity

The photoconductivity of the grown 4NP crystal was calculated using a Keithley electrometer (Model 6517B). These crystals are analyzed in the dark and photocurrent by using two room temperature test techniques. The crystal's parallel plane is filled with silver, electro-grade, and the copper wires on both sides of the sample are thin. The sample is then coupled in series with an electrometer and a DC. To shield the sample from all radiation, a 10V to 100V increase in voltage is provided to the input in the dark current calculation. A saw the appropriate dark current. The illumination from a 100W halogen lamp with tungsten foil and iodine is utilised to calculate the photocurrent. Figure 6.6 displays the 4NP crystal's dark response and image current. The figure shows that the photocurrent is greater than the dark current, which is described as positive photoconductivity, and that both currents are linear with respect to the applied voltage. A surge in light download sources may be to blame for this. When one wave contacts another, materials with positive photoconductivity can be used [21].

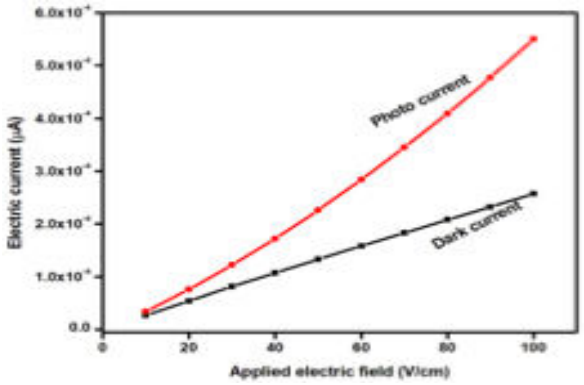

Figure 6. Photoconductivity response of 4NP crystal

3.6. TG/DTA studies

The TG and the DTA provide helpful information about the various phases of the compound phase transition and degradation. For the TG/DTA study in a nitrogen atmosphere, the SDT Q 600V 8.3 instrument was used to investigate the thermal stability of grown crystals with a heating rate of 20 °C/min from room temperature to 800 °C. Figures 6.7 show the results of the TG/DTA crystal analysis. The decomposition of a crystal occurs in a single step. This is due to the release of volatile chemicals like NO_2. At 115.5 °C, DTA experiences a significant endothermic response and offers a melting point that closely matches the compound's TG spectrum. According to the TG curve, there is no endothermic or exothermicchange below the melting point. This demonstrates that the substance is dry and stable up to 115.4°C. Volatile substances are released when temperatures exceed 115.4 °C.

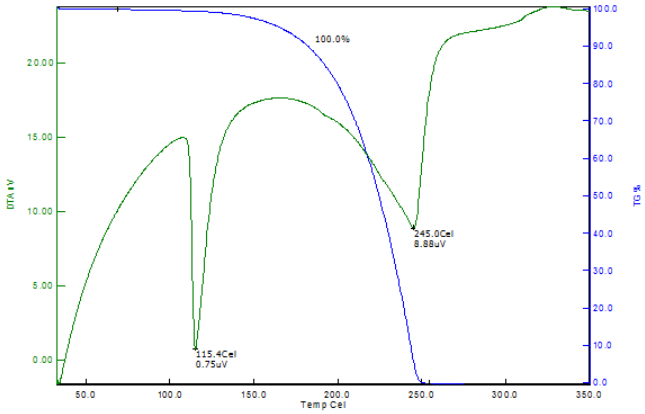

Figure 7. TG/DTA spectrum of pure 4-nitrophenol crystal

3.7. Fluorescence Studies

The photoluminescence spectrum of the grown crystals was carried out using Varian Cary Eclipse Fluorescence Spectrophotometer in room temperature. The excitation spectrum of the crystal was recorded in the range of 200-1100 nm, which is shown in Figure 8. Two bands were observed at 237 and 315 nm. Figure 9 reveals the emission spectrum. The emission peak at 420 and 442 nm attributed to blue fluorescence emission. It is observed that emission intensity suddenly decreases after 442 nm. Strong PL emission indicates that the grown crystal can be useful candidate for optoelectronic applications.

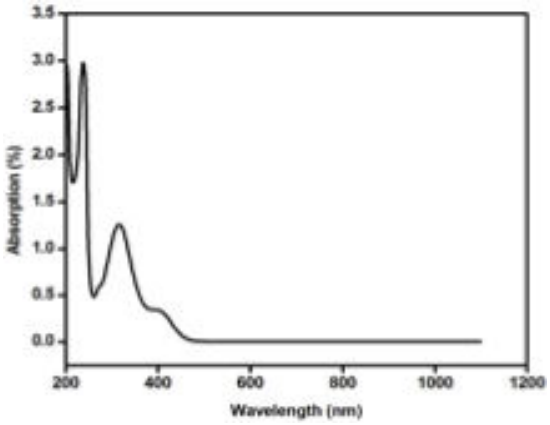

Figure 8.Excitation spectrum of 4NP crystal

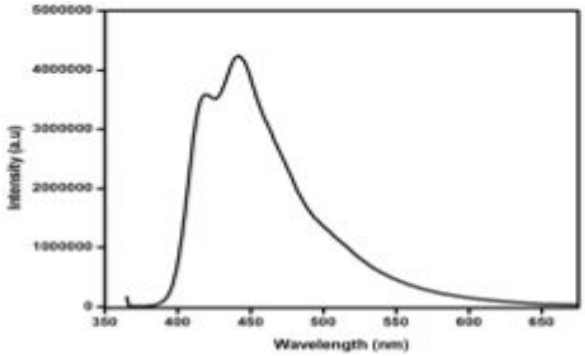

Figure 9.Emission spectrum of 4NP crystal

3.8. Powder SHG Measurement

The optical second harmonic generation behaviour of the crystal was tested by the modified Kurtz and Perry technique. The grown crystals were ground well into powder using mortar and pestle. The powder sample was densely packed in a micro capillary tube and exposed to laser radiation. High intense Q-Switched Nd:YAG laser (Quanta – Ray, spectra Physics) with output wavelength of 1064 nm is used. Frequency repetition of 10Hz and a pulse rate of 8ns were passed through the powdered sample. The SHG behaviour of the compound was confirmed from the green light emission (532 nm). The input beam energy was measured using power meter and it is 3mJ/pulse. The relative SHG signal outputs are 10 mV and 80 mV for KDP and 4NPrespectively. The optical green output was detected by a photomultiplier tube and converted into voltage output at oscilloscope. The SHG efficiency of the 4NP compound was compared to standard KDP and it is found to be 8 times greater than that of standard KDP.

3.9. Analysis of Frontier Molecular Orbitals

The two molecular orbitals that interact when discussing interacting molecular orbitals are typically the compound's Lowest Unoccupied Molecular Orbital (LUMO) and Highest Energy Occupied Molecular Orbital (HOMO). Because they are a pair in the molecule, these orbitals can interact more potently. The calculations were done in gas phase to assess the energy behaviour of the title chemical. In the gas phase, the predicted energies of the HOMO and LUMO are -0.3492 au and -0.19397 au, respectively, whereas the projected frontier orbital energy gap is 0.15523 au. Figure 10 shows the energies and surfaces of HOMO and LUMO. The material is made to be NLO active by the small intramolecular charge transfer gap that exists between HOMO and LUMO.

The energy band gap value also aids in determining a molecule's kinetic stability and chemical reactivity. The molecule's tiny band gap energy is typically associated with both high chemical reactivity and low kinetic stability. The determination of the metabolic pathways for electron transfer, photosynthesis, oxidative phosphorylation, and oxidative stress depends heavily on the ionisation energy (I) and electron affinity (A). The electrochemical oxidation potentials of the compounds have a direct relationship with the ionisation energy. The stability of free radicals and anions is estimated by their electron affinities. The ionisation energy and electron affinity can be expressed through HOMO and LUMO orbital energies by Koopmans'theorem[22]as, $I=-E_{HOMO}$ and $A=-E_{LUMO}$. From the value of ionization energy and electron affinity, Mulliken electronegativity (χ) can be calculated from the equation $\chi = (I+A)/2$. The chemical potential (μ) is the negative value of the electronegativity. Softness (S) is a property of the molecule that measures the extent of chemical reactivity. It is the reciprocal of hardness ($S= 1/2\eta$). The hardness is calculated using the expression $\eta = (I-A)/2$ (74) [23] have proposed the global

electrophilicity power of a system as, $\omega = \mu^2 / 2\eta$. This index measures the stabilisation in energy when the system acquires an additional electronic charge from the environment. The values of electronegativity, chemical hardness, softness, and electrophilicity index of the title molecule are 0.27158 eV, 0.077615 eV, 6.442 eV, and 0.47516 eV in gas phase, respectively.

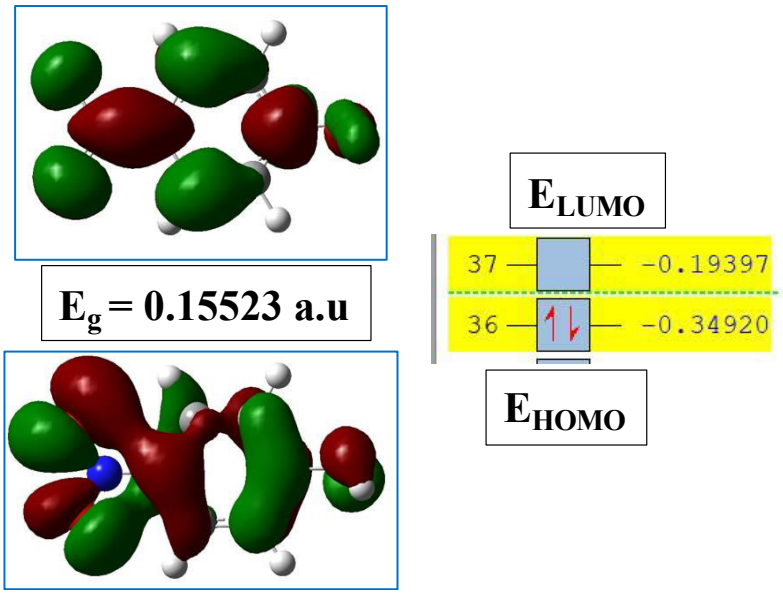

Figure 10. HOMO-LUMO of 4NP

3.10. Hyperpolarizability Study

Nonlinear Optical (NLO) effects are produced by the interactions of electromagnetic fields in different materials by changing the phase, frequency, amplitude, or other propagation characteristics of the incident fields [24,25]. One important study technique in molecular spectroscopy is the hyperpolarizability and non-linear optical characteristics of an isolated molecule of a prospective NLO material. Understanding the link between structure and property is essential for designing innovative NLO materials. One can anticipate a better description of the chemical and, as a result, more accurate findings as the basis set of the density function computation grows. In light of these considerations, the B3LYP/6-311G++(d,p) approach has been utilised to examine the crystal's hyperpolarizability. The complete equations for calculating the magnitude of the total static dipole moment (μ), mean polarizability (α), anisotropy of polarizability (Δα) and first order hyperpolarizability (β) from Gaussian output are given below

$$\mu = \sqrt{(\mu_x^2 + \mu_x^2 + \mu_x^2)}$$

$$\alpha = \frac{(\alpha_{xx} + \alpha_{yy} + \alpha_{zz})}{3}$$

$$\Delta\alpha = \sqrt{2}\left[(\alpha_{xx} - \alpha_{yy})^2 + (\alpha_{yy} - \alpha_{zz})^2 + (\alpha_{zz} - \alpha_{xx})^2 + 6\alpha_{xx}^2\right]^{1/2}$$

$$\beta = \left[\left(\beta_{xxx} + \beta_{xyy} + \beta_{xzz}\right)^2 + \left(\beta_{yyy} + \beta_{yzz} + \beta_{yxx}\right)^2 + \left(\beta_{zzz} + \beta_{zxx} + \beta_{zyy}\right)^2\right]^{1/2}$$

The polarizabilities and hyperpolarizability are reported in terms of atomic units (a.u) and the calculated values have been converted by using 1 a.u. = 0.1482 x 10^{-24} esu for α and 1 a.u. = 8.6393 x 10^{-33} cm5/esu for β. In the calculations, the values of the calculated dipole moment (μ), mean polarizability (α) and anisotropy of polarizability (Δα) are 5.3208Debye, 1.89 Å esu, 3.17 Å esu.

4. Conclusion

The slow evaporation solution growth method can be used to grow high-quality 4NP crystals at room temperature. The monoclinic system has established a single XRD glass as the grown crystal. Powder XRD demonstrated the sample's crystallinity. The structure's functional classes now use FTIR technology as well. Light transmission experiments show that transparency is greater than 90%. The sample efficiency is confirmed by the low dielectric loss value. Photo-conductivity investigations reveal crystals' advantageous characteristics. The title chemical in the powder SHG trial was 7.81 times more potent than KDP. Fluorescence experiments revealed blue fluorescence. All the findings indicate that 4NP is a viable choice for NLO applications.

5. References

1. Parr, RG, Donnelly, RA, Levy, M &Palke, WE 1978, Electronegativity the density functional viewpoint, The Journal of Chemical Physics. vol. 68, no. 03, pp. 3801-3807.
2. Evans, CC, Bagieu-Beucher, M, Massse, R &Nicoud, JF1998, Nonlinearity enhancement by solid-state proton transfer: a new strategy for the design of nonlinear optical materials, Chemistry of Materials. vol. 10, no. 01, pp. 847-854.
3. Albert Serra, RaülArtal& Maria Pozo, 2020, Jaume Garcia-Amorós and Elvira Gómez, Simple Environmentally Friendly Reduction of 4-Nitrophenol, Catalysts. vol. 10, no. 04, pp. 458-464.
4. Yuan, S, Tian, M, Cui, Y, Lin, L & Lu, X2006, Treatment of nitrophenols by cathode reduction and electro-Fenton methods. Journal of hazardous materials. vol. 137, no. 02, pp. 573–580.
5. Wang, TC, Lu, N, Li, J & Wu, Y 2011, Plasma-TiO2 catalytic method for high-efficiency remediation of p-nitrophenol contaminated soil in pulsed discharge. Journal of Environmental Science and Technology vol. 45, no. 3, pp. 9301–9307.

6. Ruan, M, Song, P, Liu, J, Li, E & Xu, W 2017, Highly Efficient Regeneration of Deactivated Au/C Catalyst for 4-Nitrophenol Reduction. The Journal of Physical Chemistry C. vol. 121, no. 02,pp. 25882–25887.
7. Luque, FJ, Lopez, JM & Orozco, M 2000, 'Perspective on Electrostatic interactions of a solute with a continuum. A direct utilization of ab initio molecular potentials for the prevision of solvent effects, Theoretical Chemistry Accounts. vol. 103, no. 2, pp. 343-345.
8. Govindarajan M, Karabacak M, Suvitha A &Periandy S 2012, FT-IR, FT-Raman, ab initio, HF and DFT studies, NBO, HOMO–LUMO and electronic structure calculations on 4-chloro-3-nitrotoluene, SpectrochimicaActa Part A: Molecular and Biomolecular Spectroscopy. vol. 89, no. 07, pp. 137-148.
9. Senthil Pandian, M, Pattanaboonmee, N, Ramasamy, P &Manyum, P 2011, Studies on conventional and Sankaranarayanan-Ramasamy method (SR) grown ferroelectric glycine phosphite (GPI) single crystals, Journal of Crystal Growth. vol. 314, no. 02, pp. 207-12.
10. Senthil Pandian, M &Ramasamy, P 2012, Sodium sulfanilatedihydrate (SSDH) single crystals grown by conventional slow evaporation and Sankaranarayanan-Ramasamy (SR) method and its comparative characterization analysis, Materials Chemistry and Physics, vol. 132, no. 02, pp. 1019-28.
11. Senthil Pandian, M, Boopathi, K, Ramasamy, P &Bhagavannarayana, G 2012, The growth of benzophenone crystals by Sankaranarayanan–Ramasamy (SR) method and slow evaporation solution technique (SEST): A comparative investigation, Materials Research Bulletin. vol. 47, no. 02, pp. 826-35.
12. Shanmugam, G, Thirupugalmani, K, Rakhikrishna, R, Philip, J &Brahadeeswaran, S 2013, Thermophysical, mechanical and dielectric studies on piperidinium p-hydroxybenzoate, Journal of Thermal Analysis Calorimeter. vol. 114, no. 02, pp. 1245-54.
13. Mary Linet, J & Jerome Das, S 2011, Optical, mechanical and transport properties of unidirectional grown L-tartaric acid bulk single crystal for non-linear application. Materials Chemistry and Physics. vol. 126, no. 01, pp. 886-90.
14. Ganesh, G, Ramadoss, A, Kannan, PS &SubbiahPandi, A 2013, Crystal growth, structural, thermal, and dielectric characterization of Tutton salt $(NH_4)_2Fe(SO_4)_2.6H_2O$ crystals. Journal of Thermal Analysis Calorimeter. vol. 112, no. 03,pp.547-54.
15. NeetiGoel, Nidhi Sinha &Binay Kumar 2013, Enhanced optical, NLO, Dielectric and thermal properties of novel sodium hydrogen phthalate single crystals doped with zinc, Optical Matter. vol. 35, no. 04,pp. 479-86.

16. Babu, J. Chandrasekaran, Balaprabhakaran, S &Ilayabarathi, P 2013, Optical, structural and electrical properties of pure and urea doped KDP crystals, Material Science, Poland. vol. 31, no. 04, pp. 151-57.
17. Krishnan, P, Gayathri, K, Bhagavannarayana, G, Gunasekaran, S &Anbalagan, G 2013, Growth, nonlinear optical, thermal, dielectric and laser damage threshold studies of semi organic crystal: Monohydrate piperazine hydrogen phosphate. SpectrochimicaActa part A. vol. 102, no. 03, pp. 379-85.
18. Prakash, M, Geetha, D & Lydia Caroline, M 2013, Synthesis, structural, optical, thermal and dielectric studies on new organic nonlinear optical crystal by solution growth technique. SpectrochimicaActa part A. vol. 107, no. 04, pp. 16-23.
19. Arjunan, S, Bhaskaran, A, Mohan Kumar, R, Mohan R &Jayavel, R 2013, Effect of Iodic Acid Dopant on the Growth and Structural, Optical, and Electrical Properties of L-Arginine Phosphate Single Crystals, Material Manufacturing Process. vol. 27, no. 02, pp. 49-52.
20. Shanmugam, G, Thirupugalmani, K, Rakhikrishna, R, Philip, J &Brahadeeswaran, S 2013, Thermophysical, mechanical and dielectric studies on piperidinium p-hydroxybenzoate, Journal of Thermal Analysis Calorimeter. vol. 114, no. 02, pp. 1245-54.
21. Von Hundelshausen, U 1971, Electrooptic effect and dielectric properties of cadmium-mercury-thiocyanate crystals, Physics Letters A. vol. 34, no. 03, pp. 405-06.
22. Milton Boaz, B & Mary NavisPriya, S, Mary J, Linet, P. Martin Deva Prasath, S. Jerome Das, 2007, Photoconductivity and dielectric studies on NLO active NPNa and NPLi single crystals. Optic Material. vol. 29, no. 04, pp. 827-32.
23. Parr, RG & Yang, W 1989, Density Functional Theory of Atoms and Molecules, Oxford University Press, New York.
24. Jose, M, Uthrakumar, R, JeyaRajendran, A & Jerome Das, S 2012, Optical and spectroscopic studies of potassium p-nitrophenolatedihydrate crystal for frequency doubling applications. SpectrochimicaActa part A. vol. 86, no. 05, pp. 495-99.
25. Kurtz, SK & Perry, TT 1968, A powder technique for the evaluation of nonlinear optical materials, Journal of Applied Physics. vol. 82, no. 02,pp. 3798–3813.